J|A|C|S COMMUNICATIONS

Published on Web 10/26/2010

Linear 6,6′-Biazulenyl Framework Featuring Isocyanide Termini: Synthesis, Structure, Redox Behavior, Complexation, and Self-Assembly on Au(111)

Tiffany R. Maher, Andrew D. Spaeth, Brad M. Neal, Cindy L. Berrie, Ward H. Thompson, Victor W. Day, and Mikhail V. Barybin*

Department of Chemistry, University of Kansas, 1251 Wescoe Hall Drive, Lawrence, Kansas 66045

Received September 10, 2010; E-mail: mbarybin@ku.edu

Abstract: The key step in accessing the title species (**5**), the first nonbenzenoid diisocyanobiaryl, involved an unexpected homocoupling of a 6-bromoazulene derivative. The reversible $2e^-$ reduction of **5** was addressed electrochemically and computationally. The shifts in energies of the $S_0 \rightarrow S_1$ and $S_0 \rightarrow S_2$ transitions for a series of related 6,6′-biazulenyl derivatives correlate with the e^--donating/-withdrawing strength of their 2,2′-substituents but follow opposite trends. Species **5** adsorbs end-on (η^1) to the Au(111) surface via one of its −NC groups to form a 2-nm-thick film. In addition, bimetallic coordination of **5**'s −NC termini can be readily achieved.

Azulene is an unusual aromatic hydrocarbon ($C_{10}H_8$) that comprises an edge sharing combination of five- and seven-membered sp^2-carbon rings. The azulenic and polyazulenic motifs constitute attractive building blocks in the design of redox addressable, optoelectronic, and conductive materials.[1–4] Unlike the frontier molecular orbitals of benzenoid aromatics, the HOMO and LUMO of azulene are not mirror related and feature mutually complementary density distributions (HOMO = Highest Occupied Molecular Orbital, LUMO = Lowest Unoccupied Molecular Orbital).[3] This leads to a remarkably low $S_0 \rightarrow S_1$ excitation energy for azulene derivatives and enables topological asymmetry in the electron and hole transport regimes for azulene-based frameworks.[1–4]

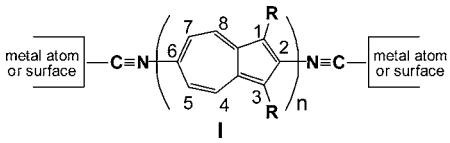

I

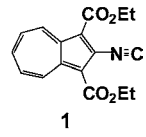

1

Coordination and surface chemistry of linear benzenoid diisocyanoarenes containing one or more linked aromatic rings has been the subject of growing experimental and theoretical interest,[5,6] particularly in the context of developing advanced materials that may support charge delocalization and transport at the nanoscale.[7] We have recently engaged in the quest for a novel class of linear diisocyanoarene linkers based on the nonbenzenoid 2,6-azulenic framework as represented by the homologous series **I**.[1,8,9] For $n = 1$ ($R = -CO_2Et$) in **I**, the orientation of the azulenic dipole can be controlled through regioselective installation and coordination of the isocyanide junction groups.[8] For $n = 2$, three different linear diisocyanobiazulenyl scaffolds can be envisioned: two symmetric featuring the 6,6′ or 2,2′ connectivity of the azulenic moieties and one asymmetric having the 2,6′ central C−C bond. Currently, very few 2,2′-, 6,6′-, and 2,6′-biazulenyl derivatives are synthetically accessible.[10] In this Communication, we introduce the chemistry of the first member of the linear diisocyanobiazulenyl family that is *formally* derived by linking two 1,3-diethoxycarbonyl-2-isocyanoazulene (**1**)[9] molecules. To the best of our knowledge, the title species is not only the first structurally characterized linear biazulenyl[10] compound but also the sole example of a crystallographically addressed biazulenyl motif of any connectivity not embedded into a larger rigid framework.[11]

Scheme 1[a]

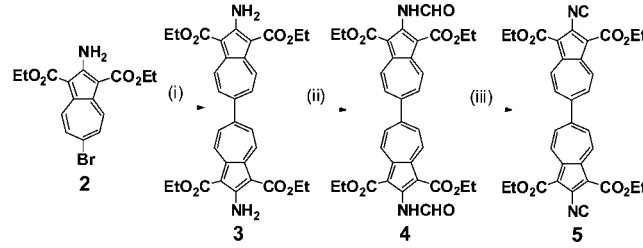

2 **3** **4** **5**

[a] (i) B_2pin_2 (0.26 equiv), 10 mol % $Pd(dppf)Cl_2 \cdot CH_2Cl_2$, KOAc, DMSO, 100 °C, argon atm.; (ii) HC(O)OAc, 50 °C, (iii) $POCl_3$, Et_3N, 20 °C.

Combining the 6-bromoazulene derivative **2**[8] with bis(pinacolato)diboron (B_2pin_2) in the presence of $Pd(dppf)Cl_2$ (dppf = bis(diphenylphosphino)ferrocene) under the conditions specified in Scheme 1 afforded brick-red 2,2-diamino-6,6′-biazulenyl **3** in a 91% yield. Surprisingly, the best yields of this unexpected, "one-pot" homocoupling of **2** were achieved by employing a substoichiometric amount (*ca.* 0.25 equiv) of B_2pin_2. No formation of **3** was observed when the reaction was conducted in the absence of B_2pin_2 under otherwise identical conditions.[12] Interestingly, our attempts to use 0.5 equiv of B_2pin_2 (the stochiometric quantity of B_2pin_2 typically employed in one-pot homocoupling of organohalides via sequential Miyaura borylation/Suzuki cross-coupling)[13] invariably led to much lower yields (≤37%) of **3**. The above quite efficient protocol for the preparation of **3** evolved from our initial efforts to improve its original synthesis by Mutafuji, Sugihara et al.[10c] The latter involved a $Pd(dppf)Cl_2$-catalyzed borylation of **2** with 1.1 equiv of B_2pin_2 to isolate the corresponding 6-azulenyl-boronic ester, which was then cross-coupled with **2** using a different catalyst, $Pd(PPh_3)_2Cl_2$, to give **3** in a 17% overall yield.[10c]

Formylation of **3** with acetic-formic anhydride afforded a 79% yield of sparingly soluble chestnut-colored 2,2′-diformamido-6,6′-biazulenyl **4**, the double dehydration of which gave lavender needles of 2,2′-diisocyano-1,1′,3,3′-tetraethoxycarbonyl-6,6′-biazulenyl **5** in a 34% isolated yield. The FTIR and ^{13}C NMR spectra of **5** exhibit signature peaks at $\nu_{C\equiv N} = 2130\ cm^{-1}$ (in Nujol mull) and $\delta = 178.6$ ppm (in $CDCl_3$), respectively, that correspond to the isocyanide termini of this air-stable compound.

It is well argued that varying the nature of the substituent in a 2-substituted azulene chiefly affects the energy of its LUMO but not HOMO.[3] The λ_{max} value for the relatively weak $S_0 \rightarrow S_1$ transition

10.1021/ja108202d

in the electronic spectra of **3**, **4**, and **5** in CH_2Cl_2 appears to increase upon proceeding from **3**[14] to **4** (474 nm) to **5** (509 nm). This trend parallels the order of decreasing e^--donating/increasing e^--withdrawing strength of the groups at the 2,2′-positions in these 6,6′-biazulenyls: NH_2 > −NHCHO > −N≡C. At the same time, however, λ_{max} of the more intense higher energy band, which we tentatively assign as $S_0 \rightarrow S_2$, increases in reverse order **5** (390 nm) < **4** (421 nm) < **3** (459 nm). Thus, the 2,2′-substitution of the 6,6′-biazulenyl scaffold provides an opportunity to simultaneously tune the wavelengths of both $S_0 \rightarrow S_1$ and $S_0 \rightarrow S_2$ excitations in mutually opposing directions in the visible region.

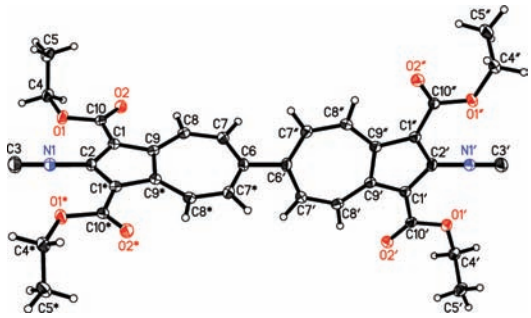

Figure 1. Molecular structure of **5** (50% thermal ellipsoids).

The solid state structure of **5** depicted in Figure 1 is remarkably symmetric with only 1/4 of the molecule being crystallographically independent. The C3−N1 bond length of 1.165(3) Å observed for **5** is typical for an isocyano N≡C triple bond.[8] Every carboxylate unit in **5** is essentially coplanar with the azulenic moiety to which it is attached. The long axis of **5** spans 17.1 Å, as defined by the C3···C3′ distance. The C6−C6′ bond connecting the azulenyl rings in **5** is 1.512(4) Å long. This distance is statistically shorter than the $C(sp^3)-C(sp^3)$ bond of 1.535(4) Å connecting the two seven-membered rings in 1,1′,6,6′-tetrahydro-6,6′-biazulene-1,1′-diide, $[H_8C_{10}-C_{10}H_8]^{2-}$,[15] but only marginally longer than the central C−C bond length documented for biphenyl (1.494(3)−1.507 Å).[16,17]

The 66.9° torsion angle between the azulenic planes in crystalline **5** is almost certainly significantly influenced by crystal packing forces. Our density functional theory (DFT) analysis of 2,2′-diisocyano-6,6′-biazulenyl (**5a**), a truncated analogue of **5** that lacks all ester substituents, predicts the equilibrium interplanar angle of 52.0° for this model compound with the barriers to internal rotation about the C6−C6′ bond to achieve the planar and orthogonal conformations being $\Delta E(0°) = 8.2$ kcal/mol and $\Delta E(90°) = 1.3$ kcal/mol, respectively. Notably, both experimental and recent DFT studies of biphenyl indicate that the $H_5C_6-C_6H_5$ molecule exhibits the torsional angle of *ca.* 45° with the rotational barriers $\Delta E(0°) \approx \Delta E(90°) \leq 2.0$ kcal/mol in the gas phase.[18] While the $\Delta E(90°)$ values for both **5a** and $(C_6H_5)_2$ are similar, the higher $\Delta E(0°)$ value for **5a** reflects greater steric congestion about the central C−C bond connecting the two seven-membered rings in the planar conformation of **5a** compared to the environment of the central C−C linkage in the planar orientation of biphenyl.

Compound **1**, the structure of which may be viewed as one-half of that of **5**, undergoes an irreversible one-electron reduction at $E_{p,c} = -1.55$ V vs Cp_2Fe^+/Cp_2Fe in CH_2Cl_2. In sharp contrast, the cyclic voltammogram (CV) of **5** in the same solvent features a nicely reversible ($i_{p,c}/i_{p,a} = 1.0$) two-electron reduction wave at the substantially less negative potential of $E_{1/2} = -1.02$ V (Figure 2). This observation echoes the reduction behavior of the "parent" 6,6′-biazulenyl addressed by Hünig and Ort in a series of their pioneering redox studies of various biazulenic motifs.[19] The persistence of $\mathbf{5}^{2-}$, at least on the electrochemical time scale, can be attributed to the closed-shell nature of its 6,6′-biazulenide dianion framework (Figure 3, left).[10b,19d,20] The singlet electronic configuration of $\mathbf{5}^{2-}$ is also suggested by our DFT examination of its model $\mathbf{5a}^{2-}$. The singlet (S) state of $\mathbf{5a}^{2-}$ is predicted to be nearly 0.7 eV less energetic than the triplet (T) state. The DFT calculations show that the reduction process $\mathbf{5a} \rightarrow \mathbf{5a}^{2-}$ (S) is accompanied by appreciable shortening of the central C−C bond, as well as by a 30° decrease in the interplanar angle between the two azulenic moieties (Table 1). The HOMO of $\mathbf{5a}^{2-}$ (S) illustrated in Figure 3 clearly implies the significant double bond character of the dianion's central C−C linkage. Similar to **5**, the CV of **3** also features one reversible reduction wave, which occurs at a more negative potential ($E_{1/2} = -1.64$ V) compared to that of **5** due to the electron-donating nature of the $-NH_2$ termini.

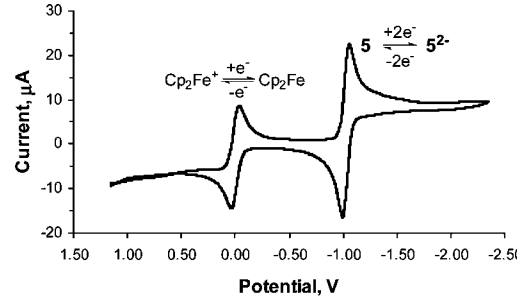

Figure 2. Cyclic voltammogram of **5** in 0.1 M $[^nBu_4N][PF_6]/CH_2Cl_2$ vs internal Cp_2Fe^+/Cp_2Fe (1 equiv) at 25 °C. Scan rate = 100 mV/s.

Figure 3. Left: bis(cyclopentadienide)-like resonance form of $\mathbf{5}^{2-}$. Right: DFT-generated HOMO of $\mathbf{5a}^{2-}$(S).

Table 1. DFT-Generated Relative Energies in the Gas Phase (ΔE_{gas}) and in Dichloromethane (ΔE_{DCM}), Interplanar Dihedral Angles (α), and the Central C−C Bond Length (*d*) for **5a**, $\mathbf{5a}^{2-}$(S), and $\mathbf{5a}^{2-}$(T)

Model species	ΔE_{gas}, eV	ΔE_{DCM}, eV	α, deg	*d*, Å
5a	0	0	52.0	1.50
$\mathbf{5a}^{2-}$(S)	−1.58	−5.92	21.9	1.43
$\mathbf{5a}^{2-}$(T)	−0.91	−5.23	58.5	1.51

The molecule of **5** can be readily used to bridge metal centers. For example, treatment of *in-situ*-generated $W(CO)_5(THF)$ with 0.5 equiv of **5** in THF provided fuchsia-colored $[(OC)_5W]_2(\mu\text{-}\mathbf{5})$ that features two "$(OC)_5W$" units linked through the 6,6′-biazulenyl bridge by means of the N≡C junctions. Complex $[(OC)_5W]_2(\mu\text{-}\mathbf{5})$ undergoes a reversible reduction at $E_{1/2} = -1.01$ V in CH_2Cl_2. This reduction potential is almost identical to that of **5** thereby indicating that the LUMO of $[(OC)_5W]_2(\mu\text{-}\mathbf{5})$ is largely bridge-based. The lowest energy band ($\lambda_{max} = 496$ nm) in the electronic spectrum of $[(OC)_5W]_2(\mu\text{-}\mathbf{5})$ can be assigned to the metal-to-bridge charge transfer (MBCT), and its molar extinction coefficient (ε) is *ca.* 35 times greater than that documented for the $S_0 \rightarrow S_1$ transition for **5**. Notably, the analogous MBCT for $[(OC)_5W]_2(\mu$-2,6-diisocyano-1,3-diethoxycarbonylazulene) has a λ_{max} value of 515 nm,[8] whereas the corresponding transition for $[(OC)_5W]_2(\mu$-1,4-diisocyanobenzene) occurs in the UV region ($\lambda_{max} = 370$ nm).[21]

Exposure of a gold-coated mica substrate to a 2 mM solution of **5** in CH_2Cl_2 without protection from air led to adsorption of **5** on

the Au(111) surface. The ellipsometric thickness of the resulting film, measured at multiple spots on the substrate, was 20.5 ± 2.4 Å. This value is consistent with the molecular monolayer nature of the self-assembled film featuring approximately parallel orientation of the long molecular axis of **5** with respect to the surface normal.[5] Indeed, for the perfectly upright η^1 coordination of **5** to the gold surface (Figure 4), the monolayer thickness can be expected to be approximately 19.1 Å. This estimate is obtained by adding 2.0 Å, a typical Au(0)−CNR bond length,[5] to the 17.1 Å distance between the two isocyanide carbon atoms in **5** (Figure 1).

The grazing incidence reflection absorption infrared (RAIR) spectrum of a freshly prepared film of **5** on Au(111) also suggests the end-on adsorption of **5** to the Au surface. Indeed, the spectrum exhibits two bands in the isocyanide stretching region (Figure 4). The higher energy band at 2170 cm^{-1} corresponds to $\nu_{C\equiv N}$ of the C≡N terminus of **5** bound to the gold surface. The broad nature of this band is typical for aryl isocyanide self-assembled monolayers (SAMs) on gold[22] and can be attributed to some inhomogeneity in the environment of the surface adsorption sites due to defects in the Au(111) film prepared via gold vapor deposition.[23] Notably, the $\nu_{C\equiv N}$ stretch for SAMs of **1** on Au(111) also occurs at 2170 cm^{-1}.[9] Since the isocyanide carbon's lone pair is antibonding with respect to the C≡N bond,[1] donation of electron density from the −NC junction to gold upon chemisorption of **5** results in a pronounced (43 cm^{-1}) blue shift in ν_{CN} for the gold-bonded isocyanide terminus of **5** relative to that of the compound in solution. Concurrently, such coordination should induce a slight positive charge[7e] within the π-system of **5**, which may lead to weakening of the C≡N bond of the unbound isocyanide group, provided there is a sufficient extent of conjugation between the two azulenyl moieties. In accord with this argument, the sharp $\nu_{C\equiv N}$ band at 2119 cm^{-1} in the RAIR spectrum in Figure 4 that corresponds to the uncoordinated −N≡C end of **5** is depressed by 8 cm^{-1} relative to $\nu_{C\equiv N}$ observed for **5** in CH_2Cl_2 solution (or by 11 cm^{-1} compared to $\nu_{C\equiv N}$ for the bulk compound in Nujol mull). Interestingly, when adsorbed on metallic gold, linear benzenoid diisocyanoarenes featuring up to three linked arylene units show 2−9 cm^{-1} red shifts in ν_{CN} for their free −N≡C end relative to ν_{CN} for the corresponding bulk substances.[22b,d]

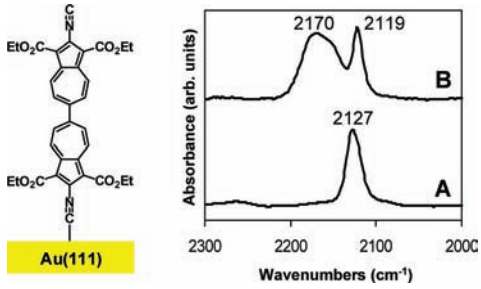

Figure 4. Left: schematic drawing of the terminal upright (η^1) bonding of **5** to the gold surface. Right: $\nu_{C\equiv N}$ regions of (A) FTIR spectrum of **5** in CH_2Cl_2 solution and (B) RAIR spectrum of a SAM film of **5** on Au(111).

The SAM of **5** described herein constitutes the first example of a molecular film involving a biazulenic scaffold. Accessibility of such SAMs presents a hitherto unavailable intriguing opportunity to experimentally probe[7] the conductivity characteristics of a 6,6′-biazulenyl-based molecular wire. Further studies advancing the coordination and surface chemistry of the 6,6′-biazulenyl and 6,6′-biazulenide frameworks are underway in our laboratory.

Acknowledgment. This work was supported by the NSF CAREER Award (CHE-0548212) and DuPont Young Professor Award to M.V.B. The authors thank Dr. Matthew Benning of Bruker AXS for collecting the X-ray diffraction data for **5** and Professors Malinakova and Tunge for helpful discussions.

Supporting Information Available: Experimental procedures; spectroscopic and analytical data; details of the electrochemical, X-ray, surface, and DFT studies (PDF and CIF). This material is available free of charge via the Internet at http://pubs.acs.org.

References

(1) Barybin, M. V. *Coord. Chem. Rev.* **2010**, *254*, 1240–1252.
(2) (a) Dias, J. R. *J. Phys. Org. Chem.* **2007**, *20*, 395–409. (b) Burdzinski, G.; Kubicki, J.; Maciejewski, A.; Steer, R. P.; Velate, S.; Yeow, E. K. L. *Mol. Supramol. Photochem.* **2006**, *14*, 1–36. (c) van der Veen, M. H.; Rispens, M. T.; Jonkman, H. T.; Hummelen, J. C. *Adv. Funct. Mater.* **2004**, *14*, 215–223. (d) Feringa, B. L.; van Delden, R. A.; Koumura, N.; Geertsema, E. M. *Chem. Rev.* **2000**, *100*, 1789–1816. (e) Treboux, G.; Lapstun, P.; Silverbrook, K. *J. Phys. Chem. B* **1998**, *102*, 8978–8980.
(3) Shevyakov, S. V.; Li, H.; Muthyala, R.; Asato, A. E.; Croney, J. C.; Jameson, D. M.; Liu, R. S. H. *J. Phys. Chem. A* **2003**, *107*, 3295–3299.
(4) For a class III mixed-valence species, in which the electronic coupling is mediated by the 2,6-azulenedicarboxylate bridge, see: Barybin, M. V.; Chisholm, M. H.; Dalal, N. S.; Holovics, T. H.; Patmore, N. J.; Robinson, R. E.; Zipse, D. J. *J. Am. Chem. Soc.* **2005**, *127*, 15182–15190.
(5) Lazar, M.; Angelici, R. J. Isocyanide Binding Modes on Metal Surfaces and in Metal Complexes. In *Modern Surface Organometallic Chemistry*; Basset, J.-M., Psaro, R., Roberto, D., Ugo, R., Eds.; Wiley-VCH: Weinheim, 2009; pp 513−556 and references therein.
(6) Selected recent theoretical reports: (a) Li, Y.; Lu, D.; Galli, G. *J. Chem. Theory Comput.* **2009**, *5*, 881–886. (b) Li, Y.; Lu, D.; Swanson, S. A.; Scott, J. C.; Galli, G. *J. Phys. Chem. C* **2008**, *112*, 6413–6421.
(7) Representative examples: (a) Choi, S. H.; Kim, B.; Frisbie, C. D. *Science* **2008**, *320*, 1482–1486. (b) Chu, C.; Ayres, J. A.; Stefanescu, D. M.; Walker, B. R.; Gorman, C. B.; Parsons, G. N. *J. Phys. Chem. C* **2007**, *111*, 8080–8085. (c) Kim, B.; Beebe, J. M.; Jun, Y.; Zhu, X.-Y.; Frisbie, C. D. *J. Am. Chem. Soc.* **2006**, *128*, 4970–4971. (d) Murphy, K. L.; Tysoe, W. T.; Bennett, D. W. *Langmuir* **2004**, *20*, 1732–1738. (e) Hong, S.; Reifenberger, R.; Tian, W.; Datta, S.; Henderson, J.; Kubiak, C. P. *Superlattices Microstruct.* **2000**, *28*, 289–303.
(8) Holovics, T. C.; Robinson, R. E.; Weintrob, E. C.; Toriyama, M.; Lushington, G. H.; Barybin, M. V. *J. Am. Chem. Soc.* **2006**, *128*, 2300–2309.
(9) DuBose, D. L.; Robinson, R. E.; Holovics, T. C.; Moody, D.; Weintrob, E. C.; Berrie, C. L.; Barybin, M. V. *Langmuir* **2006**, *22*, 4599–4606.
(10) (a) Ito, S.; Terazono, T.; Kubo, T.; Okujima, T.; Morita, N.; Murafuji, T.; Sugihara, Y.; Fujimori, K.; Kawakami, J.; Tajiri, A. *Tetrahedron* **2004**, *60*, 5357–5366. (b) Ito, S.; Okujima, T.; Morita, N. *J. Chem. Soc., Perkin Trans. 1* **2002**, 1896–1905. (c) Kurotobi, K.; Tabata, H.; Miyauchi, M.; Murafuji, T.; Sugihara, Y. *Synthesis* **2002**, 1013–1016. (d) Morita, T.; Takase, K. *Bull. Chem. Soc. Jpn.* **1982**, *55*, 1144–1152. (e) Hanke, M.; Jutz, C. *Synthesis* **1980**, 31–32.
(11) The X-ray structure of a diazuleno[2,1-*a*:1,2-*c*]naphthalene derivative, which formally contains the 1,1′-biazulenyl motif has been reported: Ito, S.; Nomura, A.; Morita, N.; Kabuto, C.; Kobayashi, H.; Maejima, S.; Fujimori, K.; Yasunami, M. *J. Org. Chem.* **2002**, *67*, 7295–7302.
(12) A small amount of an orange-brown mixture isolated after workup in this control experiment contained 1,3-diethoxycarbonyl-2-aminoazulene (the product of debromination of **2**) as one of the major constituents.
(13) Representative examples: (a) Nising, C. F.; Schmid, U. K.; Nieger, M.; Bräse, S. *J. Org. Chem.* **2004**, *69*, 6830–6833. (b) Kabalka, G. W.; Yao, M.-L. *Tetrahedron Lett.* **2003**, *44*, 7885–7887.
(14) For **3**, the $S_0 \rightarrow S_1$ band is likely obscured by the lower energy tail of the substantially more intense $S_0 \rightarrow S_2$ transition at λ_{max} = 459 nm.
(15) Bock, H.; Arad, C.; Näther, C.; Göbel, I. *Helv. Chim. Acta* **1996**, *79*, 92–100.
(16) Robertson, G. B. *Nature* **1961**, 593–594.
(17) Trotter, J. *Acta Crystallogr.* **1961**, *14*, 1135–1140.
(18) (a) Johansson, M. P.; Olsen, J. *J. Chem. Theory Comput.* **2008**, *4*, 1460–1471. (b) Bastiansen, O.; Samdal, S. *J. Mol. Struct.* **1985**, *128*, 115–125.
(19) (a) Hünig, S.; Ort, B. *Liebigs Ann. Chem.* **1984**, 1905–1935. (b) Hünig, S.; Ort, B. *Liebigs Ann. Chem.* **1984**, 1936–1951. (c) Hünig, S.; Ort, B.; Hanke, M.; Jutz, C.; Morita, T.; Takase, K.; Fukazawa, Y.; Aoyagi, M.; Ito, S. *Liebigs Ann. Chem.* **1984**, 1952–1958. (d) Hünig, S.; Ort, B. *Liebigs Ann. Chem.* **1984**, 1959–1971.
(20) Ito, S.; Okujima, T.; Morita, N.; Ohta, K.; Kitamura, T.; Imafuku, K. *J. Am. Chem. Soc.* **2003**, *125*, 1669–1680.
(21) Grubisha, D. S.; Rommel, J. S.; Lane, T. M.; Tysoe, W. T.; Bennett, D. W. *Inorg. Chem.* **1992**, *31*, 5022–5027.
(22) (a) Toriyama, M.; Maher, T. R.; Holovics, T. C.; Vanka, K.; Day, V. W.; Berrie, C. L.; Thompson, W. H.; Barybin, M. V. *Inorg. Chem.* **2008**, *47*, 3284–3291. (b) Swanson, S. A.; McClain, R.; Lovejoy, K. S.; Alamdari, N. B.; Hamilton, J. S.; Scott, J. C. *Langmuir* **2005**, *21*, 5034–5039. (c) Stapleton, J. J.; Daniel, T. A.; Uppili, S.; Cabarcos, O. M.; Naciri, J.; Shashidhar, R.; Allara, D. L. *Langmuir* **2005**, *21*, 11061–11070. (d) Henderson, J. I.; Feng, S.; Bein, T.; Kubiak, C. P. *Langmuir* **2000**, *16*, 6183–6187.
(23) Lazar, M.; Angelici, R. J. *J. Am. Chem. Soc.* **2006**, *128*, 10613–10620.

JA108202D